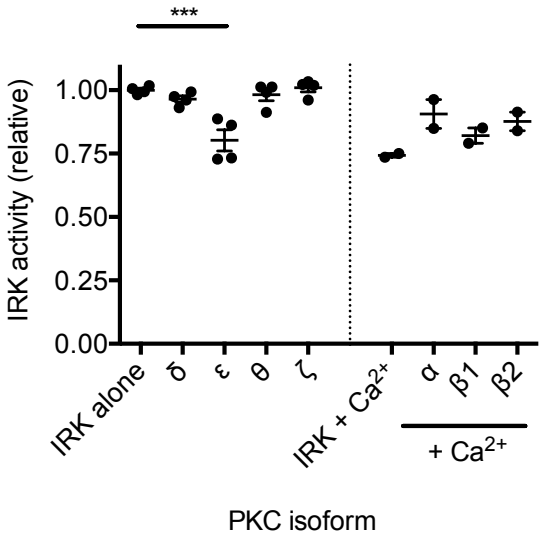

Supplemental Figure 1. PKCε is the only hepatic PKC isoform capable of inhibiting IRK activity *in vitro*.

Recombinant insulin receptor kinase domain (IRK) was pre-incubated with active recombinant PKC isoforms in equimolar ratios (10 pmol of each kinase). Subsequently, IRK tyrosine kinase activity was measured using ^{32}P incorporation into the synthetic substrate Axltide as readout. For reactions involving calcium-dependent PKC isoforms (α, β1, β2) $CaCl_2$ (10 mM) was included. Control reactions measuring IRK activity in the presence of 10 mM $CaCl_2$ were performed, revealing lower IRK activity in this reaction condition independent of cPKC activity. Intact kinase activity of all PKC isoforms was confirmed in control reactions using PKCtide as substrate (data not shown). Data are mean ± SEM of n = 2-4 technical replicates per group and are pooled from two independent experiments. *** $P < 0.0005$; comparisons by two-way ANOVA with corrections for multiple comparisons.

A

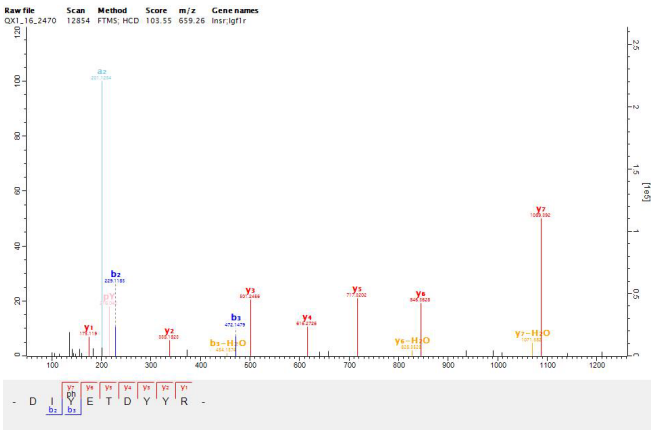

B

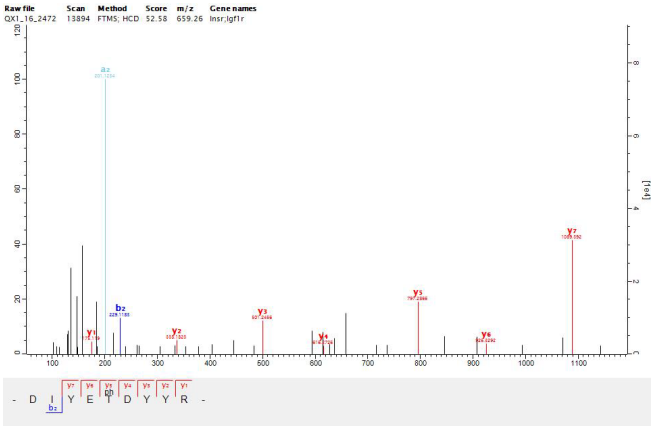

C

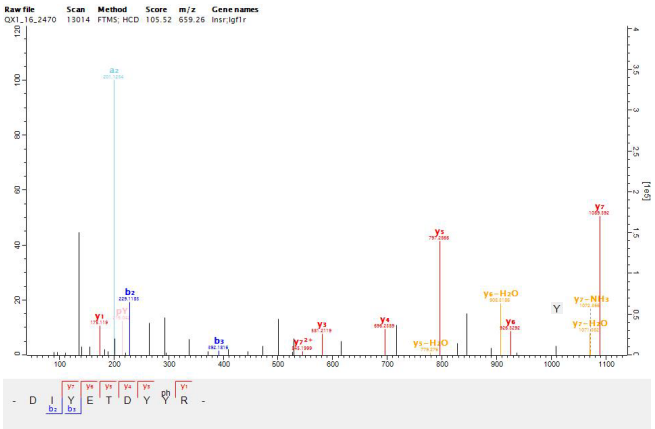

Supplemental Figure 2. Demonstration of INSR Thr^{1160} phosphorylation in intact cells. McArdle rat hepatoma cells were transiently transfected with human INSR-GFP. GFP immunoprecipitates were separated by SDS-PAGE and gel bands containing INSR-GFP were trypsin digested, phosphopeptide enriched with TiO_2, and analyzed for Thr^{1160} phosphorylation by LC-MS/MS. Peptides were identified by MaxQuant, and phosphosite localization was confirmed by manual inspection and comparison to synthetic standards. Fragment ions extracted from the spectrum shown in **Figure 2C**, demonstrating peptides phosphorylated at **(A)** Y1158, **(B)** T1160, or **(C)** Y1162.

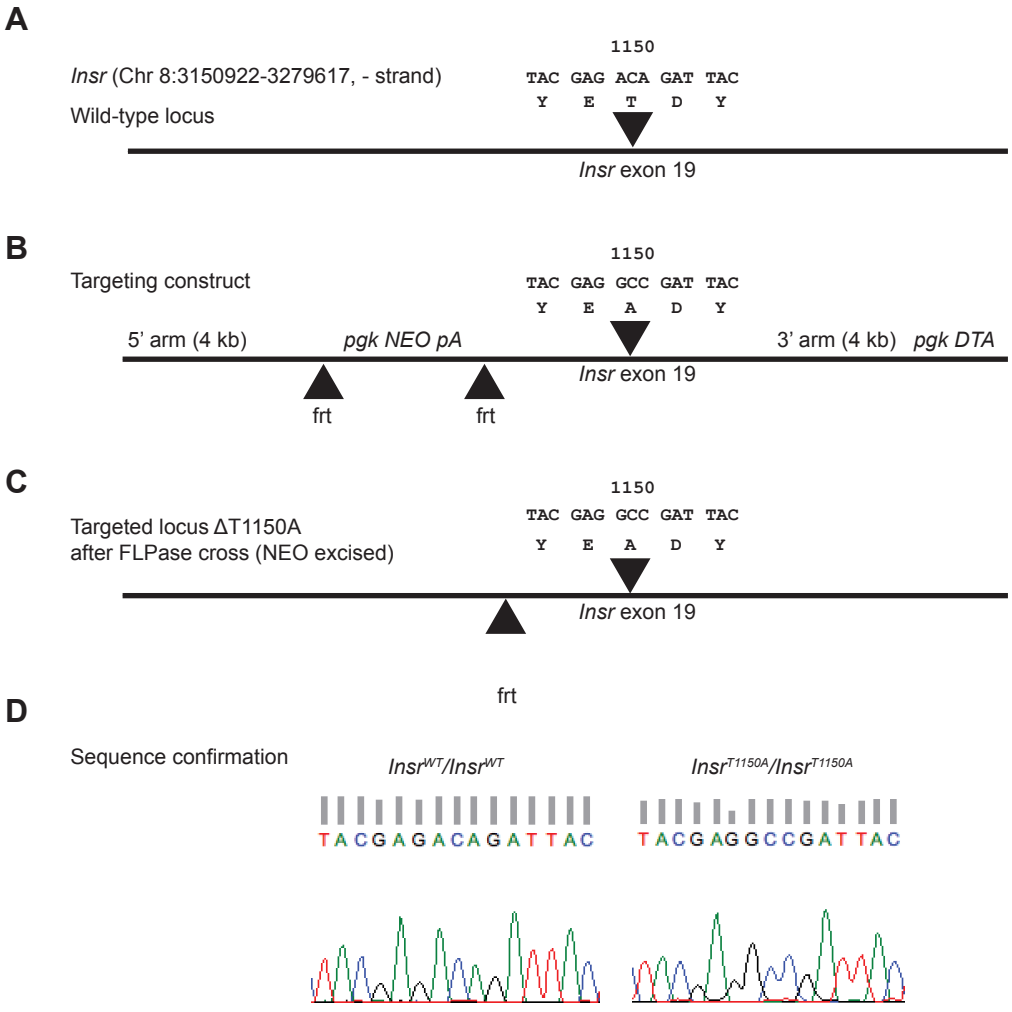

Supplemental Figure 3. Generation of *Insr*^{T1150A} mice.

(A) Schematic of wild-type mouse *Insr* locus with codons surrounding Thr^{1150}. **(B)** Targeting construct used for homologous recombination. **(C)** Mutated *Insr*^{T1150A} locus after crossing to FLPase deleter mice to excise the neomycin resistance cassette. **(D)** Representative electropherograms from wild-type (left) and littermate homozygous *Insr*^{T1150A} mice (right).

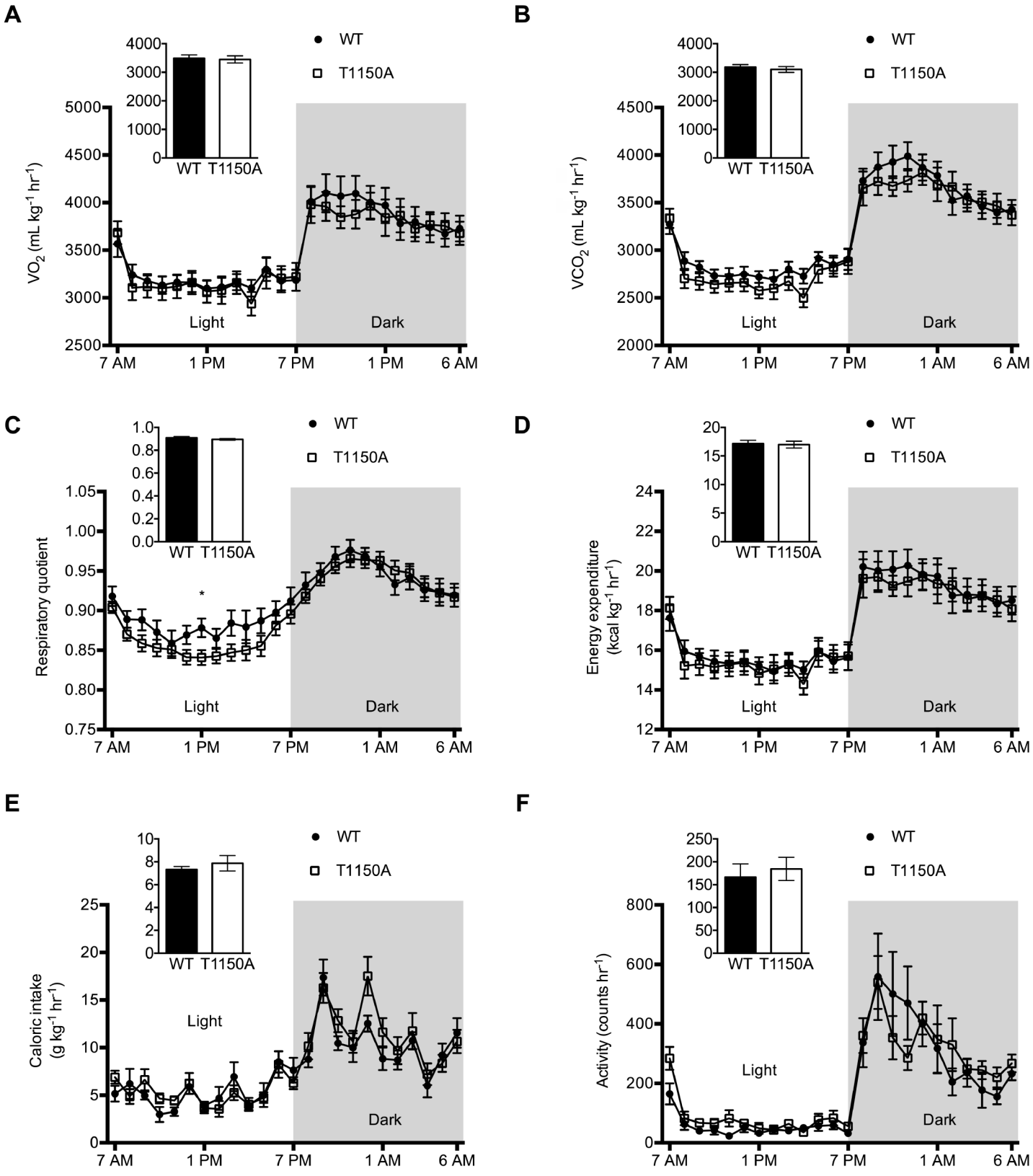

Supplemental Figure 4. Metabolic cage studies of male *Insr*^{T1150A} mice on regular chow diet.

(A) Oxygen consumption. **(B)** Carbon dioxide production. **(C)** Respiratory quotient. **(D)** Energy expenditure. **(E)** Caloric intake. **(F)** Locomotor activity. In all panels, data are mean ± SEM of n = 7-9 mice per group. Bar graphs display 24-hour means. * $P < 0.05$ by two-tailed unpaired Student's *t*-test.

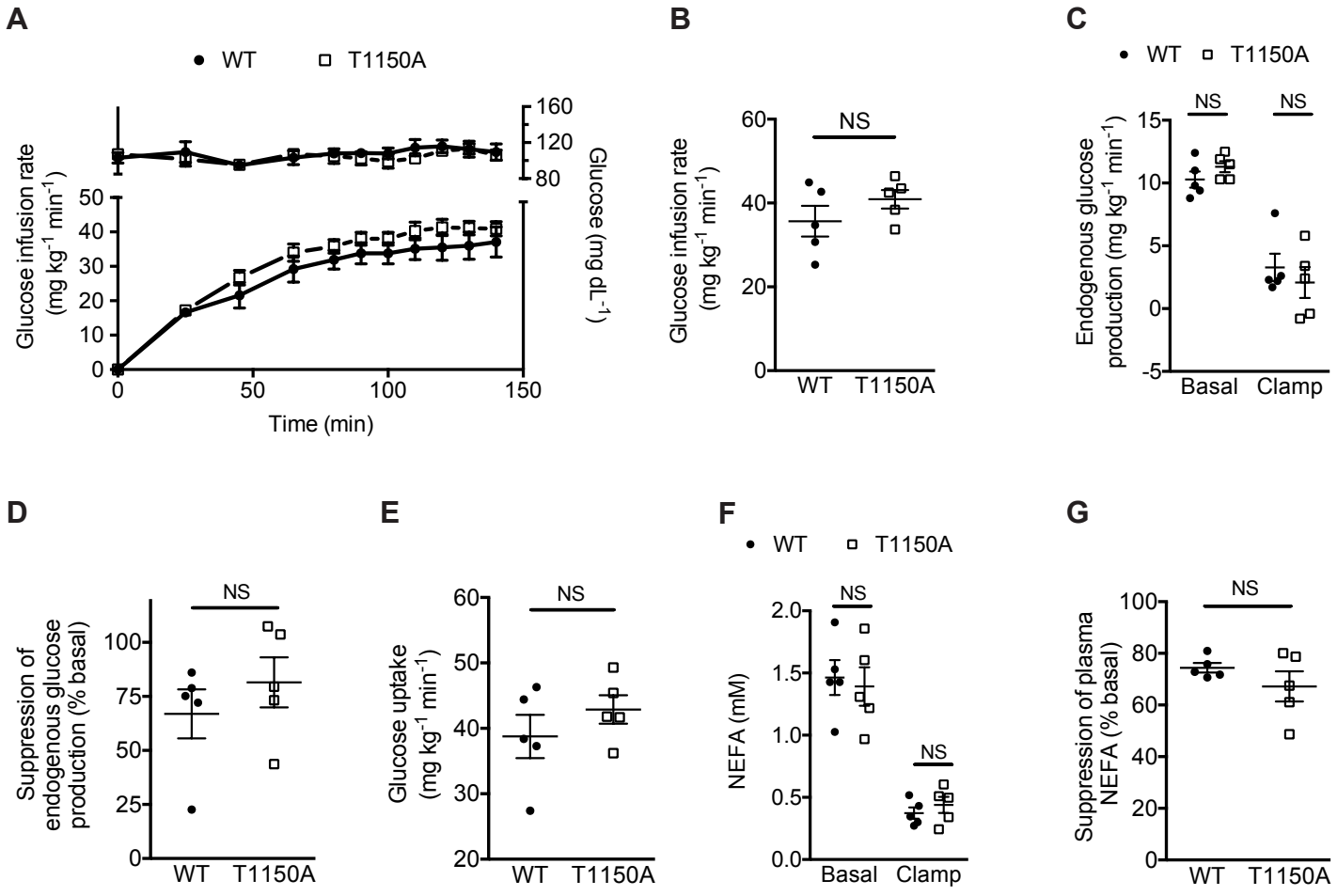

Supplemental Figure 5. *Insr*^{T1150A} mice fed regular chow diet have unaltered insulin sensitivity in hyperinsulinemic-euglycemic clamp studies.

Male *Insr*^{T1150A} or wild-type littermate mice were fed regular chow and fasted overnight before hyperinsulinemic-euglycemic clamp studies. **(A)** Time course of plasma glucose and glucose infusion rates required to achieve and maintain euglycemia. **(B)** Mean steady-state glucose infusion rates during the clamp. **(C)** Endogenous glucose production (EGP) during the basal period and during the steady-state period of the clamp. **(D)** EGP suppression during the clamp. **(E)** Peripheral glucose uptake during the steady-state period of the clamp. **(F)** Plasma nonesterified fatty acids (NEFA) during the basal period and during the steady-state period of the clamp. **(G)** NEFA suppression during the clamp. Data are mean ± SEM of n = 5 mice per group. Comparisons by two-tailed unpaired t-test.

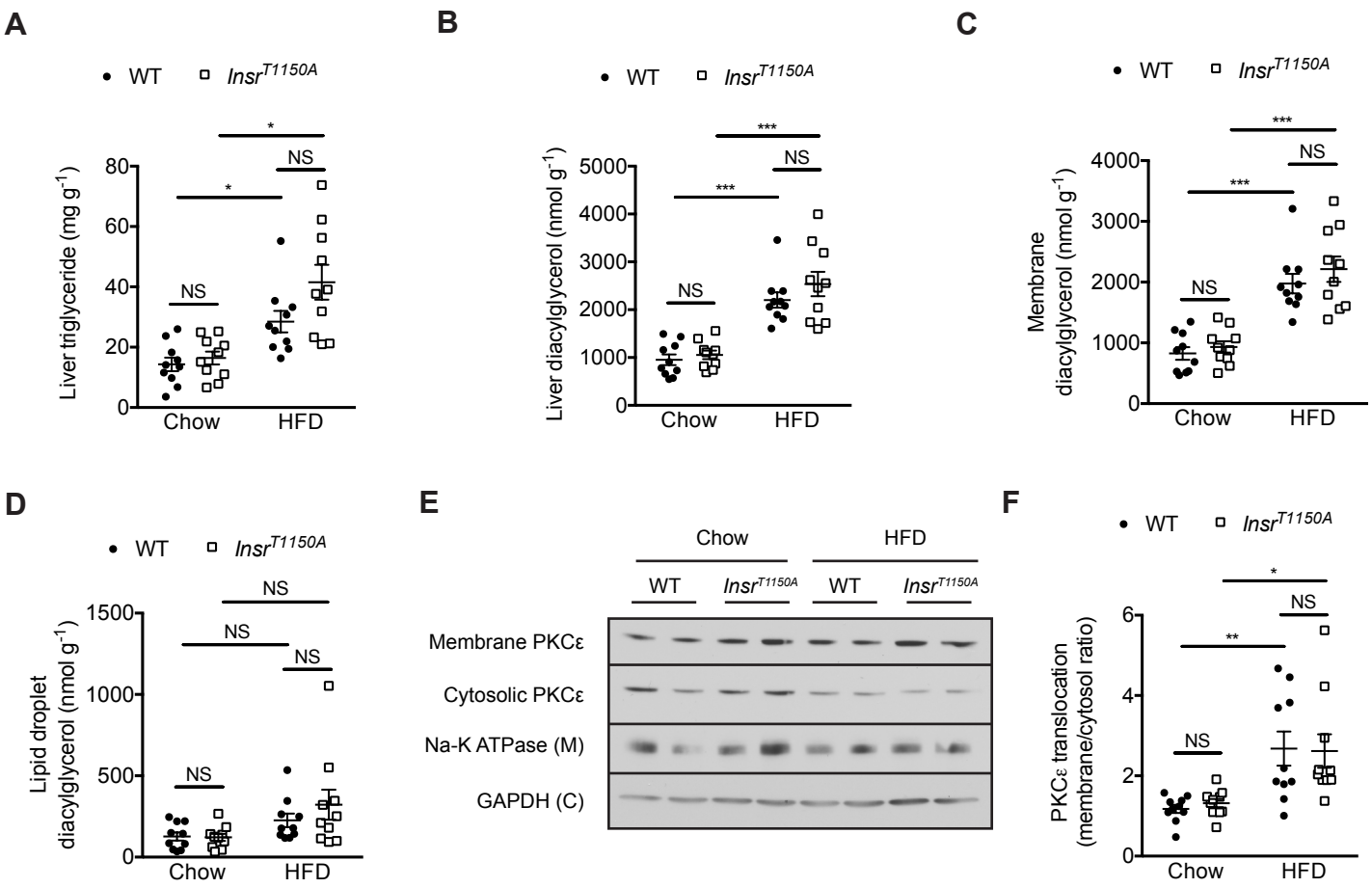

Supplemental Figure 6. *Insr*^{T1150A} mutation does not prevent hepatosteatosis and PKCε activation after short term high-fat feeding.

Male *Insr*^{T1150A} or wild-type littermate mice were fed regular chow or HFD for 8-10 d and fasted 6 h before tissue collection. **(A)** Liver triglyceride. **(B)** Liver diacylglycerol. **(C)** Diacylglycerol in the membrane-associated fraction. **(D)** Diacylglycerol in the cytosolic/lipid droplet fraction. **(E)** Representative immunoblots from PKCε translocation assay. M, membrane fraction. C, cytosolic fraction. **(F)** Quantification of PKCε translocation assay. Membrane and cytosolic PKCε intensities are normalized to Na-K ATPase and GAPDH, respectively, and the M/C ratio is calculated. Data are mean ± SEM of n = 10 mice per group. * $P < 0.05$, ** $P < 0.005$, *** $P < 0.0005$; comparisons by two-way ANOVA with corrections for multiple comparisons.

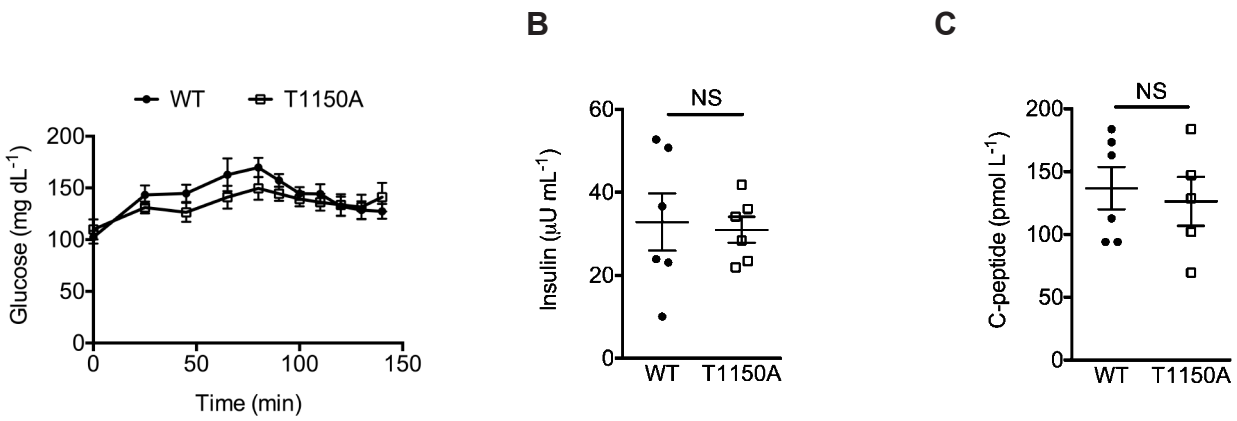

Supplemental Figure 7. Improved liver insulin signaling in *Insr*^{T1150A} mice was not attributable to increased plasma insulin levels.

Male *Insr*^{T1150A} or wild-type littermate mice were fed HFD for 8-10 days and fasted overnight before hyperinsulinemic-euglycemic clamp studies. Plasma **(A)** glucose time course. Plasma **(B)** insulin and **(C)** C-peptide levels at the end of the clamp. Data are mean ± SEM of n = 6 mice per group. Comparisons by two-tailed unpaired t-test.

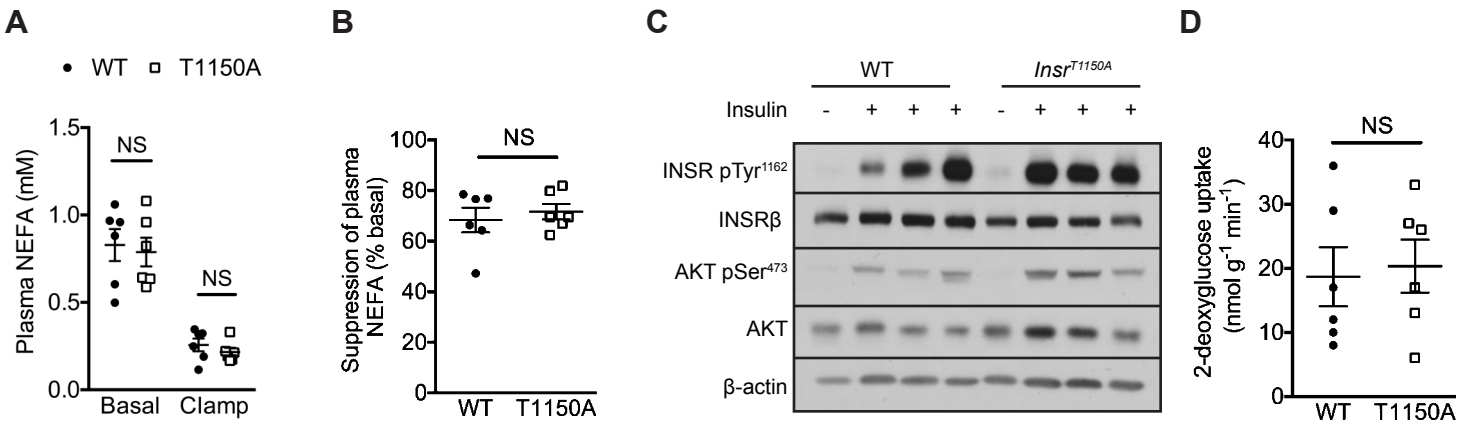

Supplemental Figure 8. Insulin action in white adipose tissue was not improved in *Insr*^{T1150A} mice fed a short term HFD.

Male *Insr*^{T1150A} or wild-type littermate mice were fed HFD for 8-10 days and fasted overnight before hyperinsulinemic-euglycemic clamp studies. **(A)** Plasma nonesterified fatty acid (NEFA) levels during the basal period and at the end of the clamp. **(B)** Suppression of plasma NEFA levels during the clamp, expressed as % basal. **(C)** INSR and AKT phosphorylation in white adipose tissue of overnight fasted (- insulin) or post-clamp (+ insulin) mice. **(D)** White adipose tissue 2-deoxyglucose uptake during the steady-state period of the clamp. In **(A-B, D)**, data are mean ± SEM of n = 6 mice per group. Comparisons by two-tailed unpaired t-test.

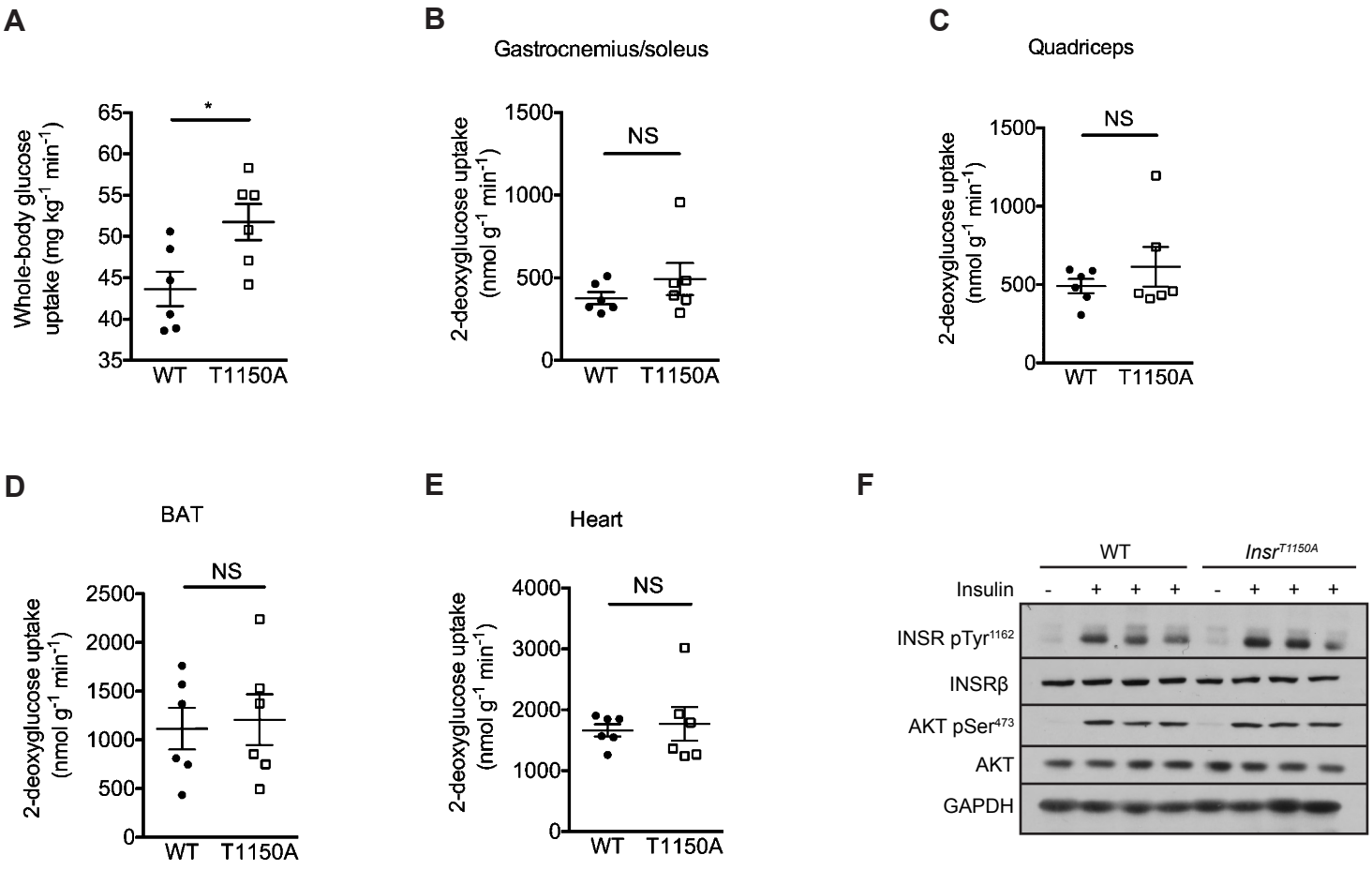

Supplemental Figure 9. Tissue-specific glucose uptake and skeletal muscle insulin signaling were not increased in *Insr*^{T1150A} mice fed a short term HFD.

Male *Insr*^{T1150A} or wild-type littermate mice were fed HFD for 8-10 days and fasted overnight before hyperinsulinemic-euglycemic clamp studies. **(A)** Whole-body glucose uptake during the steady-state period of the clamp. **(B-E)**, 2-deoxyglucose uptake during the steady-state period of the clamp in **(B)** gastrocnemius/soleus, **(C)** quadriceps, **(D)** brown adipose tissue, and **(E)** heart. **(F)** INSR and AKT phosphorylation in gastrocnemius/soleus of overnight fasted (- insulin) or post-clamp (+ insulin) mice. In **(A-F)**, data are mean ± SEM of n = 6 mice per group. * $P < 0.05$; comparisons by two-tailed unpaired t-test.

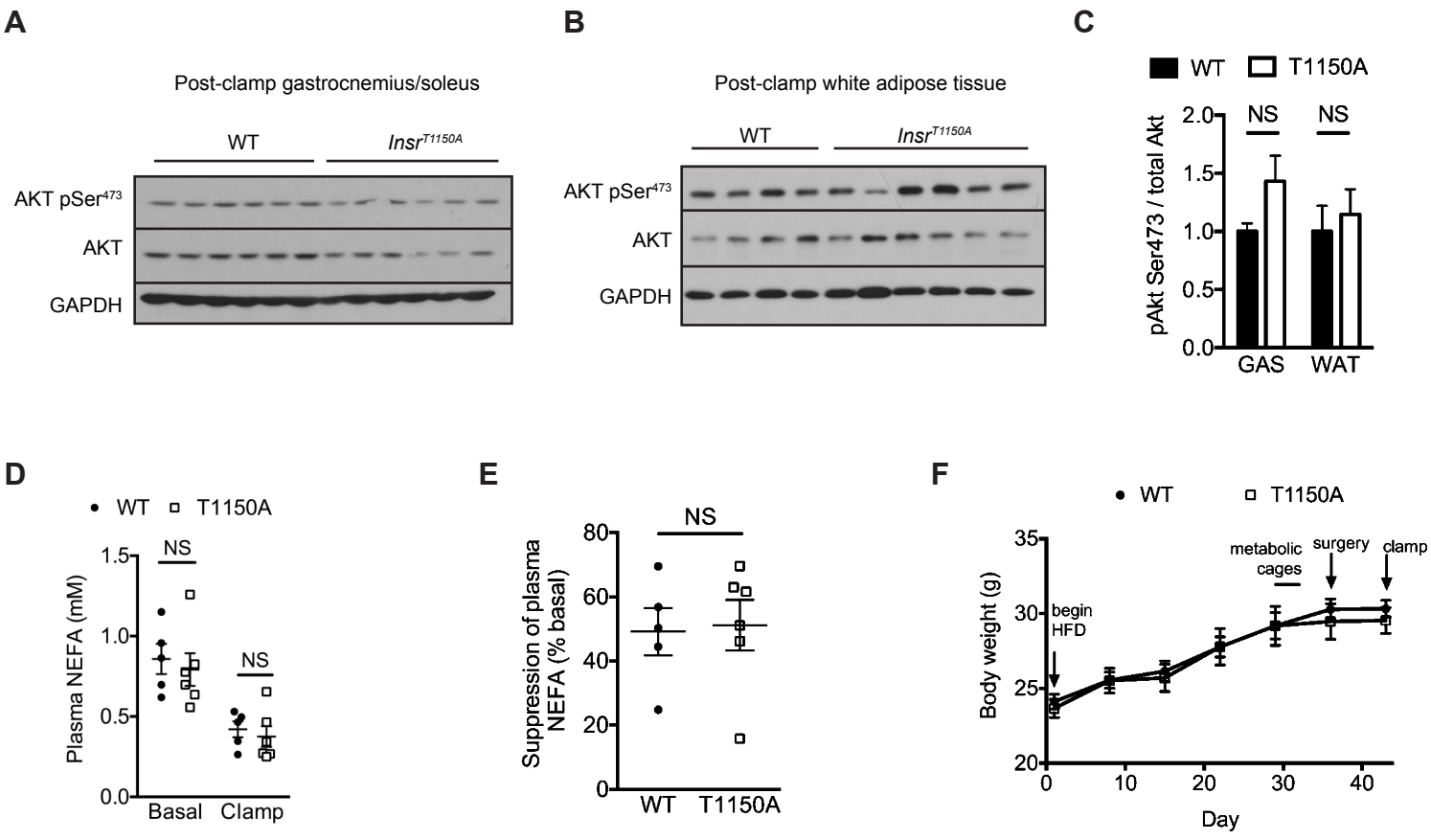

Supplemental Figure 10. *Insr*^{T1150A} mice fed a chronic HFD are not protected from adipose insulin resistance or obesity.

Male *Insr*^{T1150A} or wild-type littermate mice were fed HFD for 6 weeks and fasted overnight before hyperinsulinemic-euglycemic clamp studies. **(A-B)** AKT phosphorylation in post-clamp gastrocnemius/soleus (A) and white adipose tissue (B) lysate. **(C)** Densitometric quantification of (A) and (B). **(D)** Plasma nonesterified fatty acid (NEFA) levels during the basal period and at the end of the clamp. **(E)** Suppression of plasma NEFA levels during the clamp, expressed as % basal. **(F)** Body weight changes and experimental protocol during the 6 week HFD. Data are mean ± SEM of n = 4-7 mice per group. Comparisons by two-tailed unpaired t-test.

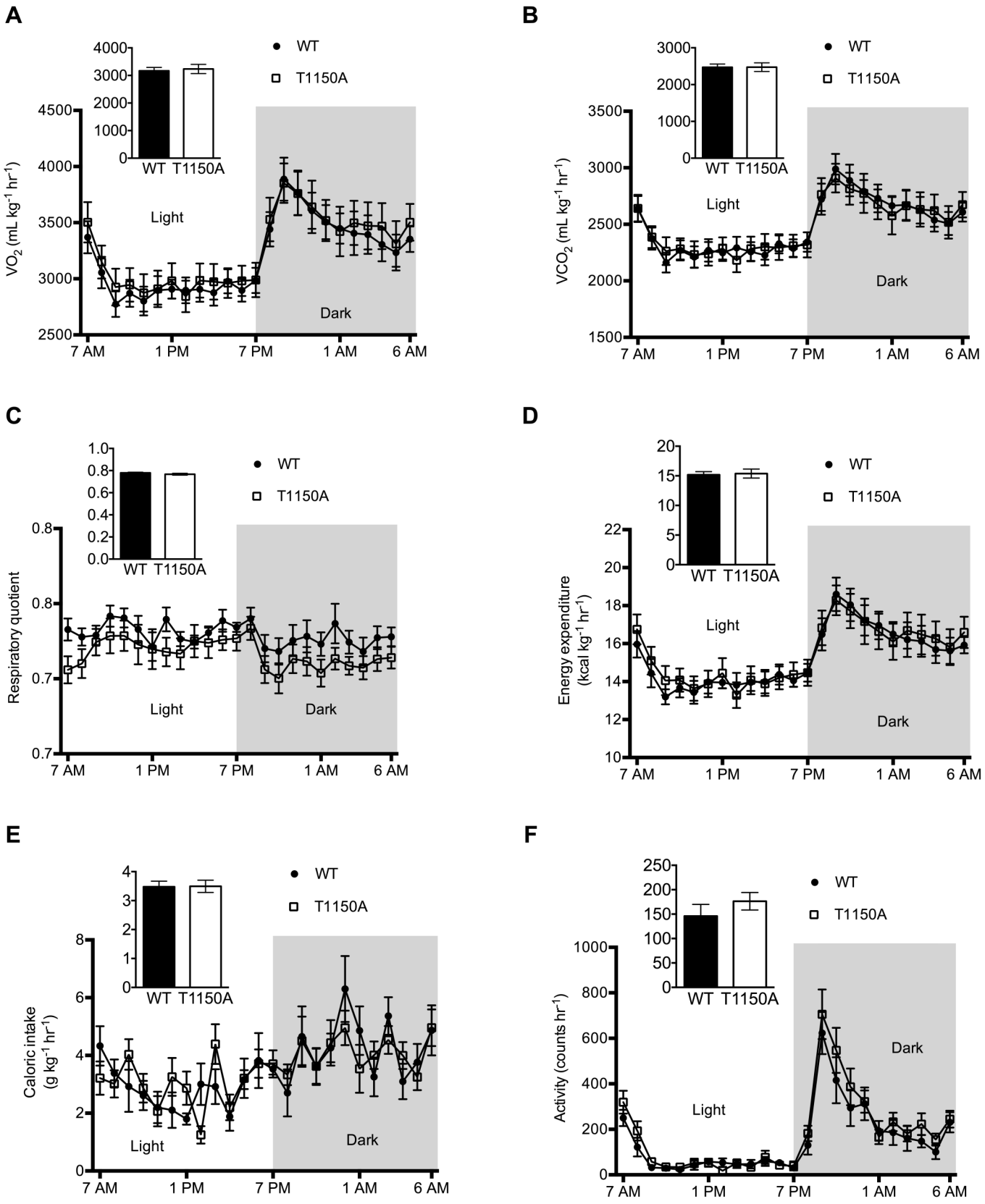

Supplemental Figure 11. Metabolic cage studies of male *Insr*^{T1150A} mice fed high-fat diet.

Male *Insr*^{T1150A} or wild-type littermate mice were fed HFD for 4 weeks before metabolic cage studies. **(A)** Oxygen consumption. **(B)** Carbon dioxide production. **(C)** Respiratory quotient. **(D)** Energy expenditure. **(E)** Caloric intake. **(F)** Locomotor activity. In all panels, data are mean ± SEM of n = 7-9 mice per group. Bar graphs display 24-hour means.

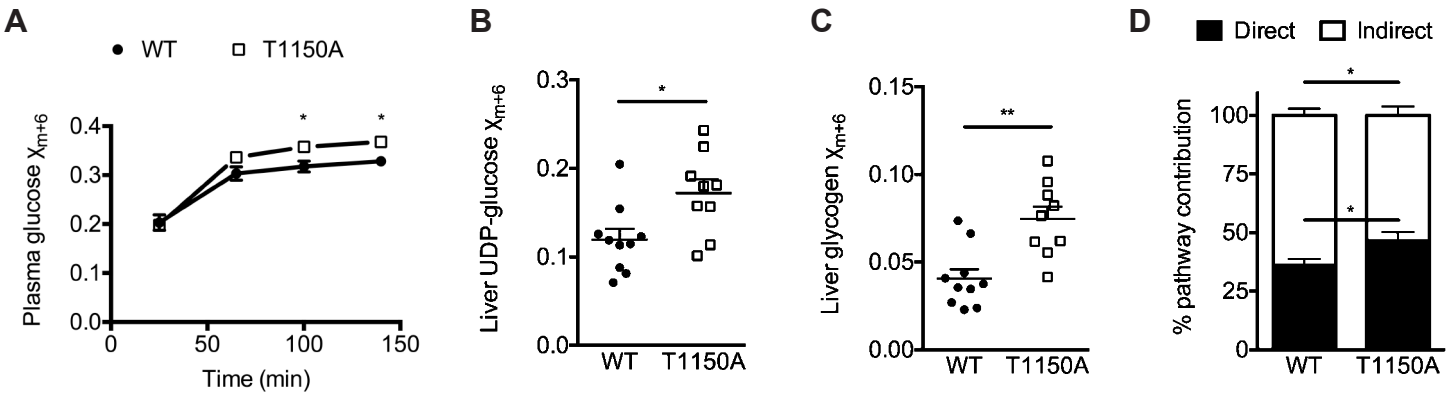

Supplemental Figure 12. Glycogen synthesis in *Insr*^{T1150A} mice during hyperinsulinemic-hyperglycemic clamp studies.

Mice were fed HFD for 8-10 days and fasted 13 h before hyperinsulinemic-hyperglycemic clamp studies. **(A)** Time course of plasma [U-^{13}C]-glucose enrichment. **(B)** *m*+6 mole fraction in liver UDP-glucose after the clamp. **(C)** *m*+6 mole fraction in liver glycogen after the clamp. **(D)** Pathway contributions to hepatic glycogen synthesis during the clamp, expressed as % of total. Data are mean ± SEM of n = 9 WT and 10 T1150A mice per group. * $P < 0.05$, ** $P < 0.005$; all comparisons by two-tailed unpaired t-test.

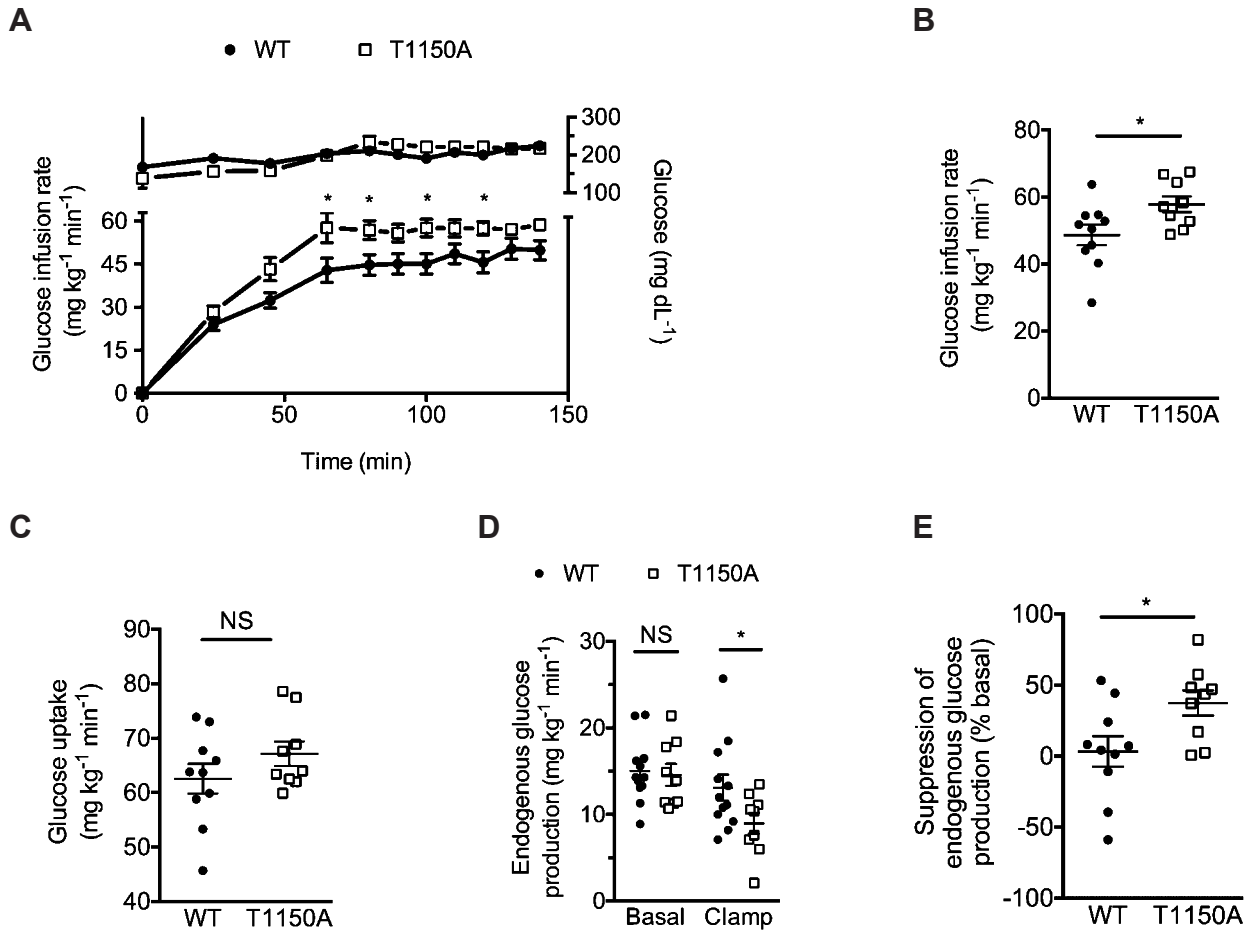

Supplemental Figure 13. Hyperinsulinemic-hyperglycemic clamp studies of *Insr*^{T1150A} mice.

Mice were fed HFD for 8-10 days and fasted 13 h before hyperinsulinemic-hyperglycemic clamp studies. **(A)** Time course of plasma glucose and glucose infusion rates required to achieve and maintain hyperglycemia. **(B)** Mean steady-state glucose infusion rates during the clamp. **(C)** Peripheral glucose uptake during the steady-state period of the clamp. **(D)** Endogenous glucose production (EGP) during the basal period and during the steady-state period of the clamp. **(E)** EGP suppression during the clamp. Data are mean ± SEM of n = 9 WT and 10 T1150A mice. * $P < 0.05$; all comparisons by two-tailed unpaired t-test.

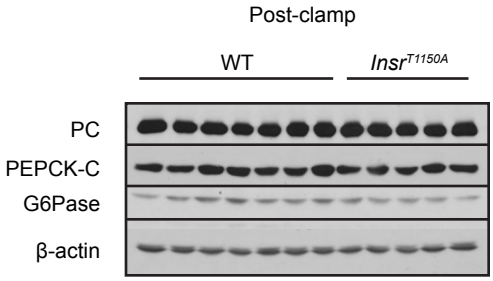

Supplemental Figure 14. Gluconeogenic protein expression in hyperinsulinemic-hyperglycemic clamp studies of *Insr*^{T1150A} mice.

Mice were fed HFD for 8-10 days and fasted 13 h before hyperinsulinemic-hyperglycemic clamp studies. Protein extracts from post-clamp livers were subjected to immunoblotting. Expression of the gluconeogenic enzymes pyruvate carboxylase (PC), cytosolic phosphoenolpyruvate carboxykinase (PEPCK-C), and glucose-6-phophatase (G6Pase). β-actin is included as a loading control.

	Wild-type	*Insr*^{T1150A}	*P*-value
N	5	5	
Age (weeks)	16.4 ± 1.1	16.2 ± 0.8	0.89
Fed body weight (g)	26.3 ± 1.0	25.5 ± 0.7	0.53
Fasted body weight (g)	23.0 ± 0.7	22.1 ± 0.5	0.35
Adiposity (%)	5.7 ± 0.5	7.2 ± 0.6	0.06
Basal plasma glucose (mg/dL)	103 ± 6	107 ± 5	0.62
Basal plasma insulin (μU/mL)	4.5 ± 0.5	6.2 ± 0.2	0.04
Clamp plasma glucose (mg/dL)	113 ± 8	108 ± 4	0.61
Clamp plasma insulin (μU/mL)	32.7 ± 2.7	45.3 ± 2.8	0.01

Supplemental Table 1. Hyperinsulinemic-euglycemic clamp studies in *Insr*^{T1150A} mice fed regular chow diet.

Male *Insr*^{T1150A} or wild-type littermate mice were fed regular chow and fasted overnight before hyperinsulinemic-euglycemic clamp studies. Data are mean ± SEM. Comparisons by two-tailed unpaired t-test.

	Chow		HFD	
	Wild-type	***Insr*^{T1150A}**	**Wild-type**	***Insr*^{T1150A}**
N	7	7	16	17
Body weight (g)	23.0 ± 0.7	24.5 ± 0.8	26.5 ± 0.5	26.4 ± 0.6
Plasma glucose (mg/dL)	194 ± 10	169 ± 13	200 ± 7	185 ± 9
Plasma insulin (μU/mL)	19.1 ± 2.9	20.2 ± 3.7	28.0 ± 2.5	24.4 ± 3.0
Plasma triglyceride (mg/dL)	44 ± 5	63 ± 12	48 ± 2	55 ± 3
Plasma NEFA (mEq/L)	0.94 ± 0.09	1.31 ± 0.19	0.76 ± 0.05	1.01 ± 0.08
Total cholesterol (mg/dL)	116 ± 6	119 ± 6	144 ± 6	147 ± 8
HDL cholesterol (mg/dL)	55 ± 3	60 ± 2	64 ± 1	63 ± 3
LDL cholesterol (mg/dL)	1.6 ± 0.2	1.4 ± 0.2	3.9 ± 0.5[a]	3.1 ± 0.5

Supplemental Table 2. Plasma parameters in 6h-fasted *Insr*^{T1150A} mice.

Male *Insr*^{T1150A} or wild-type littermate mice were fed regular chow or high-fat diet for 8-10 days and fasted 6 h before plasma and tissue collection. Data are mean ± SEM. Two-way ANOVA comparing each group to all other groups with Holm-Sidak correction for multiple comparisons was performed.
[a]$P < 0.05$ for WT chow vs WT HFD.